We are IntechOpen, the world's leading publisher of Open Access books Built by scientists, for scientists

4,800
Open access books available

122,000
International authors and editors

135M
Downloads

154
Countries delivered to

Our authors are among the

TOP 1%
most cited scientists

12.2%
Contributors from top 500 universities

CLARIVATE ANALYTICS
BOOK CITATION INDEX
INDEXED

WEB OF SCIENCE™

Selection of our books indexed in the Book Citation Index
in Web of Science™ Core Collection (BKCI)

Interested in publishing with us?
Contact book.department@intechopen.com

Wireless Body Area Networking: Joint Physical-Networking Layer Simulation and Modeling

Mojtaba Fallahpour

Additional information is available at the end of the chapter

Abstract

An electronic device equipped with sensors and antennas is the main part of the wireless body area networking (WBAN). Such a device is placed near human body and it usually works in a populated environment with many surrounding objects (e.g., building walls). The human body and the objects can change the radiation characteristics of the antenna and impact the performance of the wireless communication system. The wireless communication system's performance is also affected by the networking layers established on top of the physical layer. Therefore, any designing method for WBAN application should be pervasive, offering a joint physical-networking layer simulation and modeling strategy. To this end, in this chapter, a comprehensive simulation and modeling method is presented. First, antenna design limitations and challenges for wireless body area networking are studied with emphasis on evaluating the antenna's performance near the human body. Then, the antenna miniaturization techniques to reduce the antennas' dimension are reviewed. Later, a system level analysis and modeling are used to study short-range communication between the wearable antennas with remote nodes using IEEE 802.11g wireless networking protocol.

Keywords: wearable antenna, miniaturization, modeling, WBAN

1. Introduction

The growing interest in using connected sensors for health-care related medical diagnoses and screening demands a proper communication backbone to establish wireless body area networking (WBAN). Miniaturized electronic devices touching or placed very close to the human body are essential parts of the WBAN. These devices are equipped with sensors and

can collect data about different health-related parameters (e.g., blood sugar) in real-time [1–4]. The collected data are processed by the device itself or transmitted to another device (node) or cloud for further processing and decision-making. In order to have communication between the devices, several networking layers should be established and optimized. The physical layer is responsible for delivering data (digital bits) from sender to the destination. This backbone layer includes hardware (i.e., transmitter, receiver and antenna) and propagation medium (or channel). Other layers are built over this layer and create the connectivity and ability to communicate. The antenna is vital for wireless communication. The antenna's performance is dictated by several factors including its electrical length (physical length normalized to the operating wavelength) and the surrounding medium. For the antennas working in the microwave regime, the wavelength is measured in the centimeter scale, and so the minimum antenna dimension is usually limited to a few centimeters. On the other hand, available integrated circuit design technologies allow the whole electronics section (including sensors and processing units) to be made as small as a few millimeters. This clearly shows that the antenna is currently a bottleneck for developing small size wireless devices for WBAN.

In this chapter, first, antenna design limitations and challenges for wireless body area networking are studied with emphasis on evaluating the antenna's performance near the human body. Several antenna miniaturization techniques are reviewed, which can be used to reduce the antennas' dimension.

Later, a system-level analysis and modeling are invoked to study short-range communication between the wearable antennas with remote nodes using IEEE 802.11 g wireless networking protocol.

2. Wearable antennas

Designing a small size, flexible, body conformal, and biocompatible antenna is critical for WBAN applications. Achieving a reasonable gain (and efficiency) while reducing the antenna's dimensions is challenging [5–8]. Here, design and optimization of a typical patch antenna on a flexible PCB and its performance near the human body is studied. Three different human body models are considered: a planar slab with homogenous material (Model 1), multilayered (Model 2) and the whole-body model (Model 3).

2.1. Modeling the human body

The human body is made of different materials with different electrical (e.g., dielectric constant (permittivity) and conductivity), physical (e.g., thickness) and mechanical (e.g., compressibility, mass density) properties. Most of the electronic devices are relatively small and therefore the area directly in contact or near the device is the most influential part. Hence, the simplest model for a human body to be used for studying the electromagnetic wave interaction can be

a homogenous dielectric slab. The dielectric constant for the slab is calculated by performing an averaging on the dielectric properties of the different parts (i.e., skin, fat, muscle, etc.). This model is shown in **Figure 1(a)** and is called Model 1.

Considering the simplicity of Model 1, it may not completely capture and model the wave propagation inside a human body. Hence, a four-layer model is also included in this study (**Figure 1(b)**). The first (exterior) layer is skin, the second layer is fat, and the third layer is tissue. Depending on which part of the body is investigated, more layers including organs (e.g., heart or kidney) or bone can be added to the model. Thickness of layers is represented as $t_{layer\ name}$. This model is referred to as Model 2.

Modeling the whole body with all the details and features is computationally costly, but sometimes is needed (e.g., to evaluate the interaction of multiple devices installed on different parts of the body). The human body's electrical properties are usually frequency dependent and can significantly change at the microwave/millimeter wave regimes. Hence, characterizing and predicting these behaviors are vital for modeling purposes. Fortunately, in the recent years, there has been a great progress in this regard, and the electrical properties of different organs and tissues are included in commercial simulation tools such as ANSYS HFSS [9]. ANSYS's available 3D human body models (**Figure 2(a)**) include internal organs (e.g., the lung). For these simulations, the wearable antenna is placed outside the body, and to avoid the computational complexity during the simulations, the model with homogenous average material is used and referred to as Model 3 (**Figure 2(b)**).

(a)   (b)
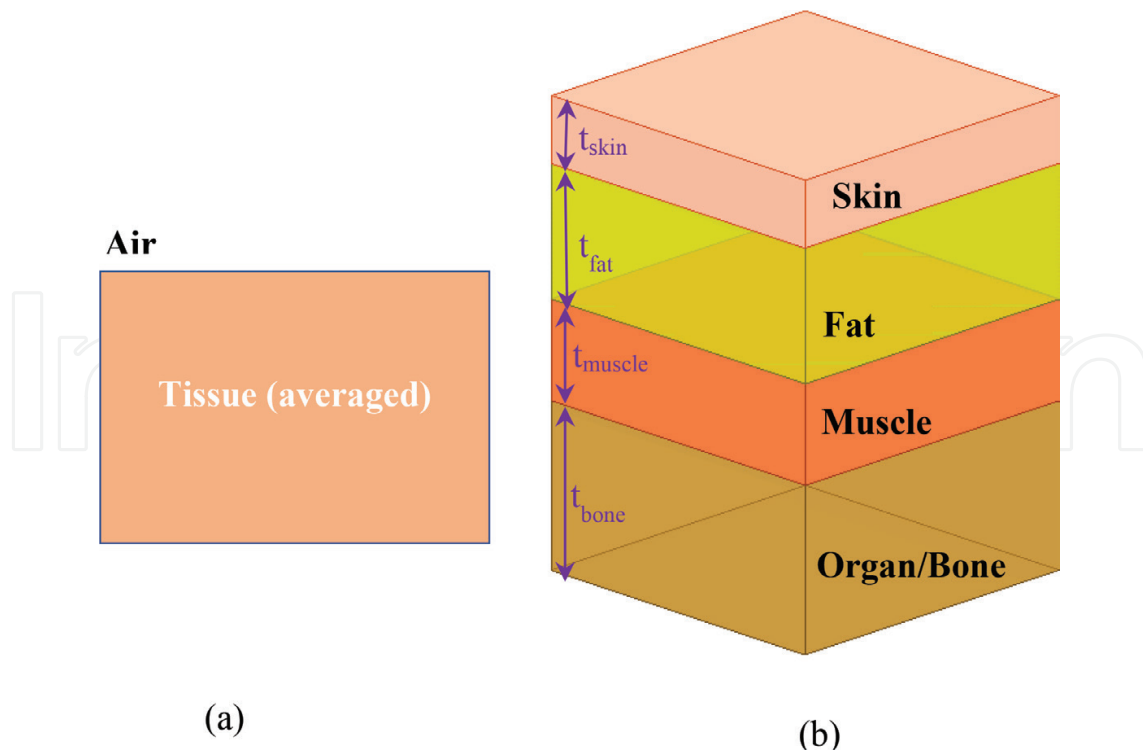
Figure 1. Flat models for human body: (a) model 1: homogenous dielectric slab and (b) model 2: multilayered structure.
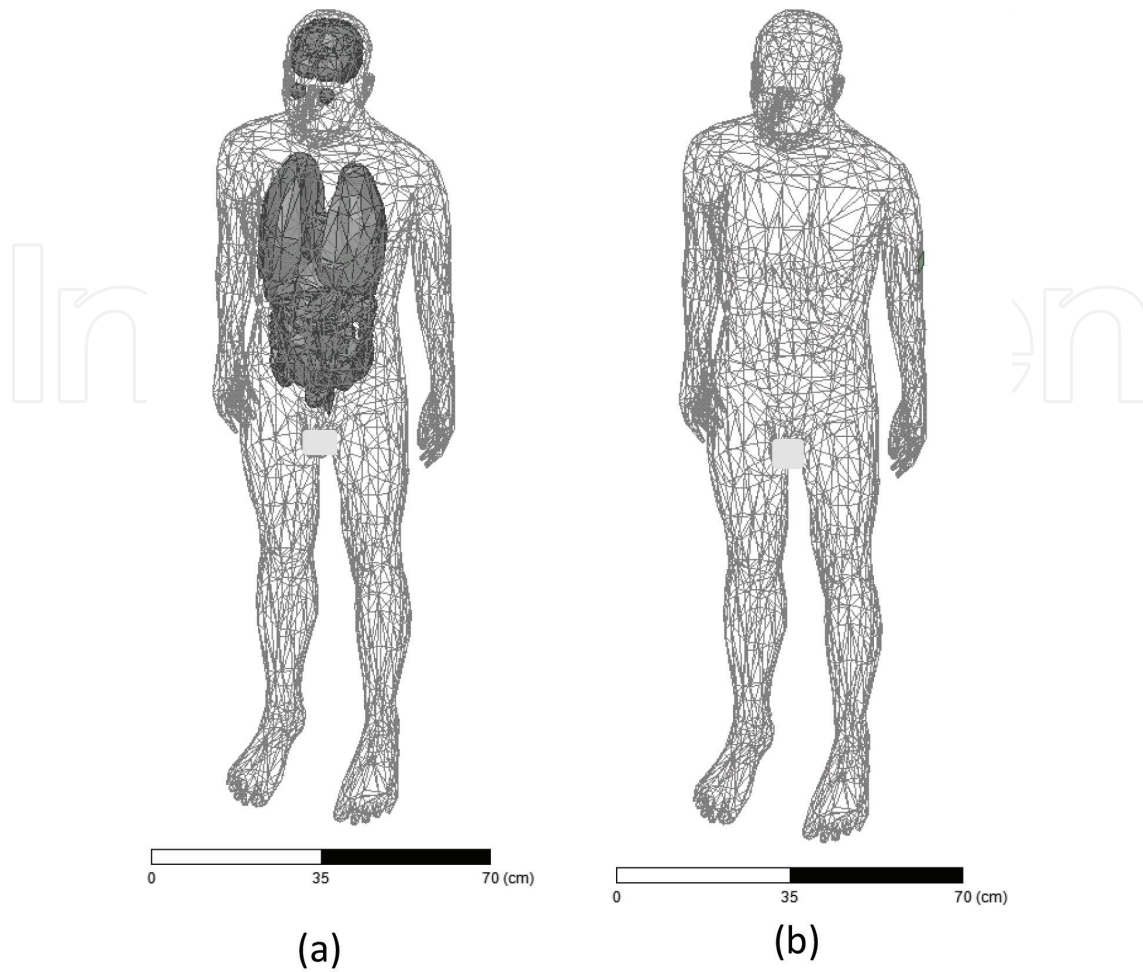
Figure 2. Human body models included in ASNSY HFSS (version R18.2). (a) Complete model with internal organs and (b) model 3: homogenous model.

2.2. Wearable antenna placement

For the wearable antennas placed near the body (skin), the electrical contrast between the human body and air results in wave reflections. Hence, the human body can load the radiating antenna and change its performance. The radiation pattern, gain, and radiation efficiency are some of the main radiation characteristics which define the antenna's performance. In the following case study, the patch antenna's performance near the human body is studied.

2.2.1. Flexible patch antenna: design and evaluation

The patch antenna is popular among antenna engineers because of its ease of fabrication and integration with planar geometries. The recent development of flexible printed circuits (FPCs) makes it possible to create wearable conformal patch antennas [10]. In this section, design and evaluation of a patch antenna operating at 2.4 GHz and implemented on a FPC will be studied. The geometry of the antenna is shown in **Figure 3**. Double sided FPC polyamide film material is selected for the antenna implementation. The substrate thickness (h) is 1 mm and its dielectric constant and dielectric loss tangent are $\varepsilon_r = 4.3$ and $\tan\delta = 0.004$, respectively.
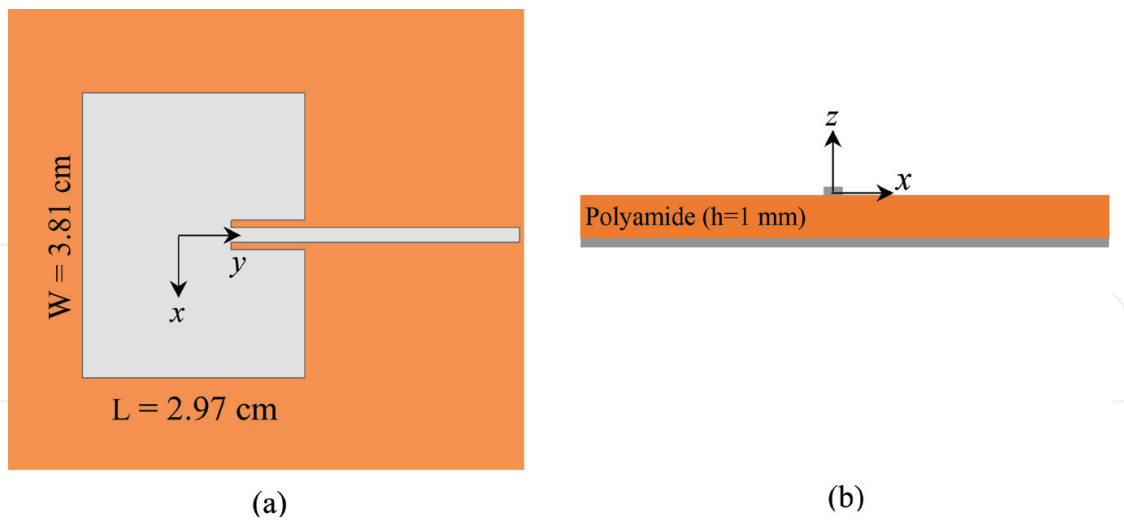
Figure 3. Designed patch antenna on FPC polyamide film material: (a) front view and (b) side view.

The patch antenna with edge feeding was initially designed to operate in free-space. To achieve the desired matching at 2.4 GHz, ANSYS HFSS was used to model, simulate, tune and optimize the dimensions and feed line location and configuration (listed in **Figure 3**). The antenna's input impedance matching to 50 Ω reference impedance, presented as the reflection coefficient (S_{11}), is plotted in **Figure 4**, which shows a good impedance matching at 2.4 GHz. The antenna's radiation gain pattern (3D) is shown in **Figure 5(a)**. The peak realized
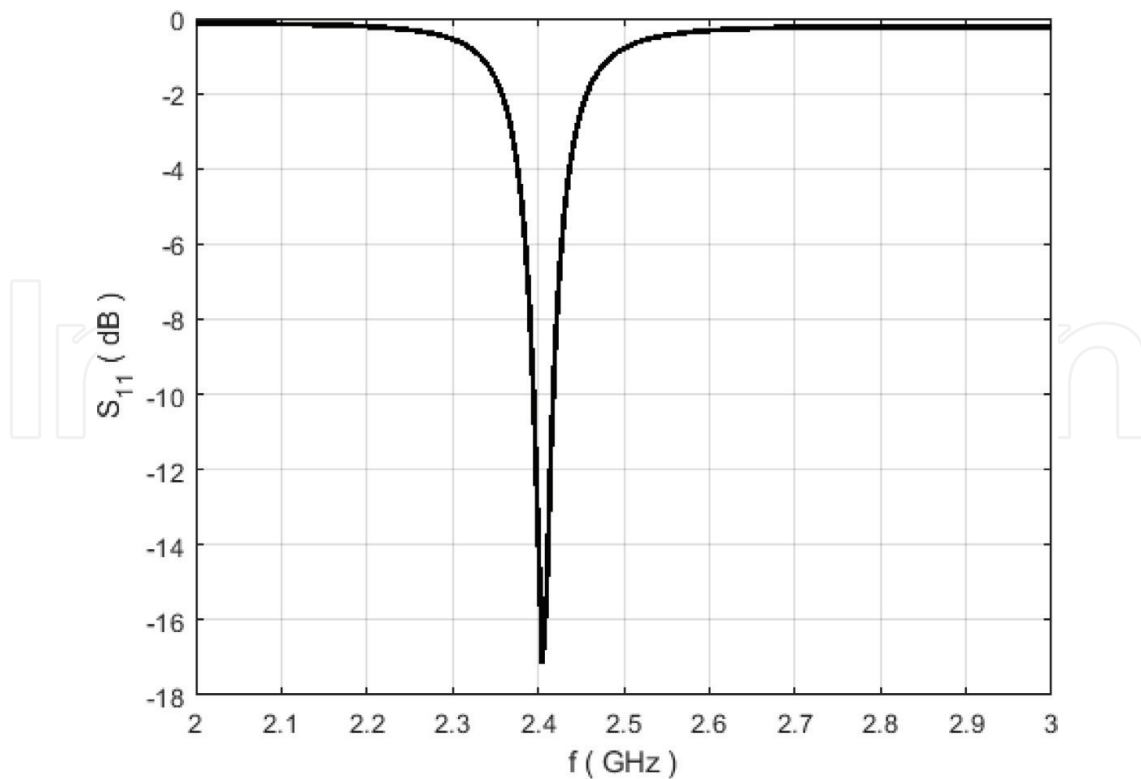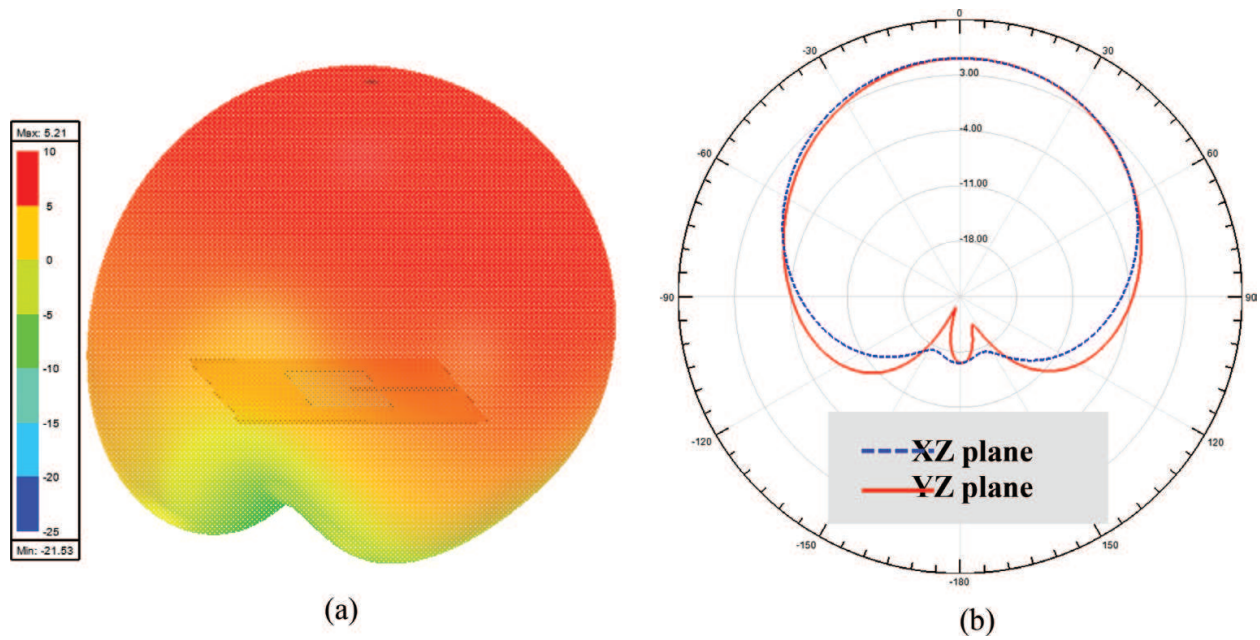

Figure 4. Calculated return loss for the flexible patch antenna from HFSS simulation.

Figure 5. Patch antenna's radiation gain pattern: (a) 3D view and (b) polar plot at XZ and YZ planes (scale: dB).

gain value (including matching loss) is 3.24 dB and the radiation efficiency is 71%. Moreover, the radiation pattern at two orthogonal planes XZ and YZ is extracted from the 3D plot and shown in **Figure 5(b)**. The plots show that the antenna has a directional beam pointing to the forward direction. Therefore, the front to back ration (F/B) for the radiation pattern is relatively high (21 dB). The antenna's characteristics are summarized in **Table 1**.

In the second step, the antenna was placed near the human body (stand-off distance of 4 mm), where Model 1 was used to represent the human body (ε_r = 28.5, σ = 3 S/m). The overall radiation performance is slightly impacted and changed (see **Table 1**). In fact, the human body acted as a large lossy reflector, and reflected the energy, resulting in a more directional beam.

Later, the antenna was placed on a four-layer model (Model 2) with stand-off distance of 4 mm and the performance was investigated. The layer properties were set as dry skin (ε_r = 36, t_{skin} = 0.1 cm), fat (ε_r = 5.27, t_{fat} = 0.5), muscle (ε_r = 52.6, t_{muscle} = 4 cm) and bone (ε_r = 18.4, t_{bone} = half-space extension). The antenna's radiation performance is summarized in **Table 1**. Like the previous case, there are some slight changes.

Configuration	f (GHz)	Realized gain (dB)	Radiation efficiency (%)	F/B ratio (dB)
Antenna in free-space	2.4	3.24	71	21
Antenna near Model 1	2.4	4.82	65	19
Antenna near Model 2	2.4	4.76	61	27
Antenna near Model 3	2.4	4.22	61	26

Table 1. Comparing the designed patch antenna's performance for different scenarios.
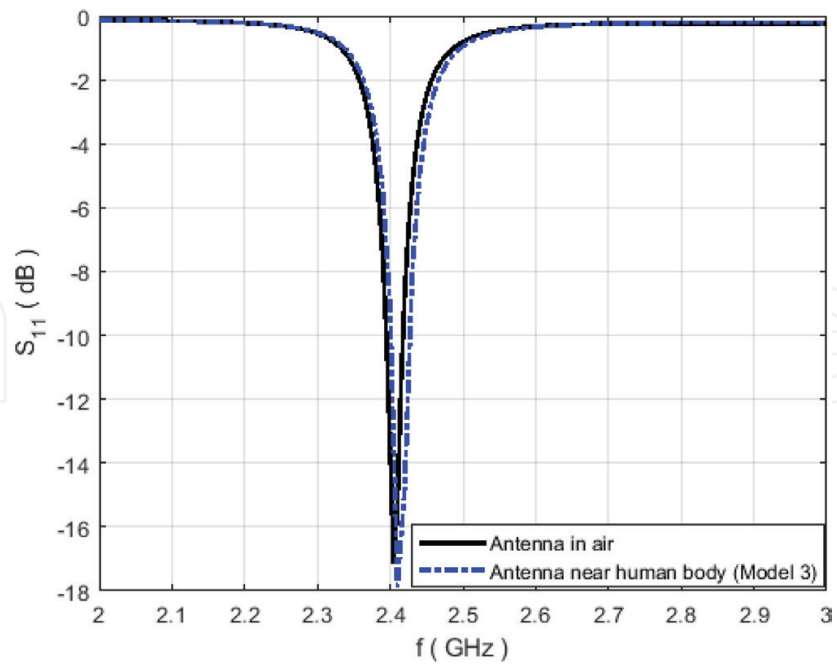
Figure 6. Simulated return loss for the flexible patch antenna placed on the left arm of the human body model (model 3) compared with the results for the antenna placed in air.
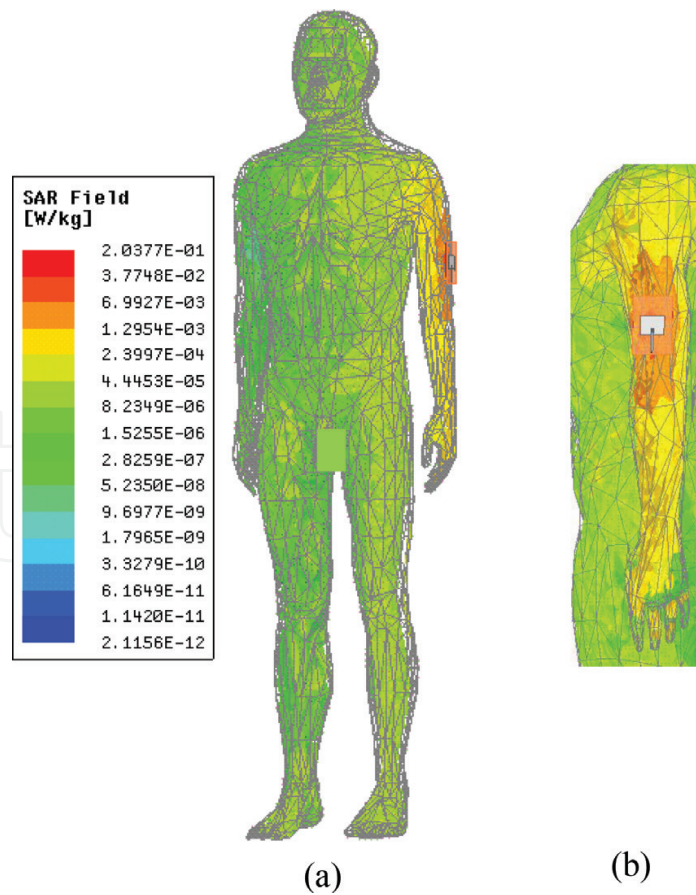
Figure 7. HFSS simulated average SAR distribution (W/kg) at 2.4 GHz (total absorbed power of 0.9 mW), (a) full-view, (b) selected left hand with the radiating antenna.

Finally, the antenna was placed on the left arm of the human body (Model 3) and its performance was investigated using the HFSS simulation tool and the results are listed in **Table 1**. The resonance frequency is shifted from 2.4 GHz to 2.41 GHz (**Figure 6**), but the overall performance of the antenna at 2.4 GHz is still acceptable.

From a safety point of view, the amount of heat generated by the antenna radiation is usually reported in term of the specific absorption rate (SAR). For the current example, the calculated average SAR is presented in **Figure 7**. There are different safety regulations and limits imposed by different countries. For example, in the United States, "the Federal Communications Commission (FCC) limit for public exposure from cellular telephones is an SAR level of 1.6 watts per kilogram (1.6 W/kg)" [11]. All wireless device manufacturers should obey this regulation. For the current example, for 10 mW available power from source, 8.80 mW was accepted by the patch antenna. From this 8.8 mW, 5.4 mW radiated, and 3.4 mW was dissipated in term of heat by the antenna and human body. The simulation results show that 0.9 mW was absorbed by the body and 2.5 mW was dissipated by the antenna itself.

3. Antenna miniaturization

Size reduction (beside conformality) is one of the main challenges in designing wearable antennas. In this section, some of the antenna miniaturization techniques will be reviewed.

Miniaturization techniques: In general, an antenna's properties and characteristics can be modified by altering its geometry, current density distribution, materials and electrical dimensions [5–7]. The antenna characteristics are usually defined in terms of input impedance matching, radiation pattern, gain, polarization, efficiency, quality (Q)-factor, and band width. In the past several decades, antenna miniaturization methods have been developed that efficiently modify and optimize the shape and the overall geometry of an antenna in order to achieve the desired characteristics while limiting the overall dimensions to be as small as possible. The miniaturization methods can be divided into topology-based and material-based methods. The topology-based techniques mainly focus on finding proper topology (e.g., geometry) for the antenna to improve its characteristics, while the material-based techniques usually achieve the desired characteristics by changing the antenna's materials (e.g., using high dielectric constant substrates). Each category has several members. Some of them are discussed here, but a more complete discussion can be found in [5].

(A) **Meander antennas:** Meander antennas aim to efficiently fill the available space by bending a long line to create a current distribution with proper phase and amplitude variations (**Figure 8**) [5]. The antenna's resonance frequency can be lowered by adding more bending to a fixed straight line. However, the radiation performance (e.g., peak gain) may decrease as a result of meandering. This is mainly because the arms can carry opposing currents whose radiation cancel each other in the far field region. Moreover, by increasing the length, the ohmic loss may increase. Meander antennas are used in commercial products due to their compactness and low manufacturing cost. As an example, meander antennas are used to design miniaturized ultra-high frequency (UHF) radio frequency identification (RFID) tags [12]. These tags are becoming popular in WBAN applications [13]. Overall, applying the meandering concept to design wearable antennas can help reduce the size of the antenna.
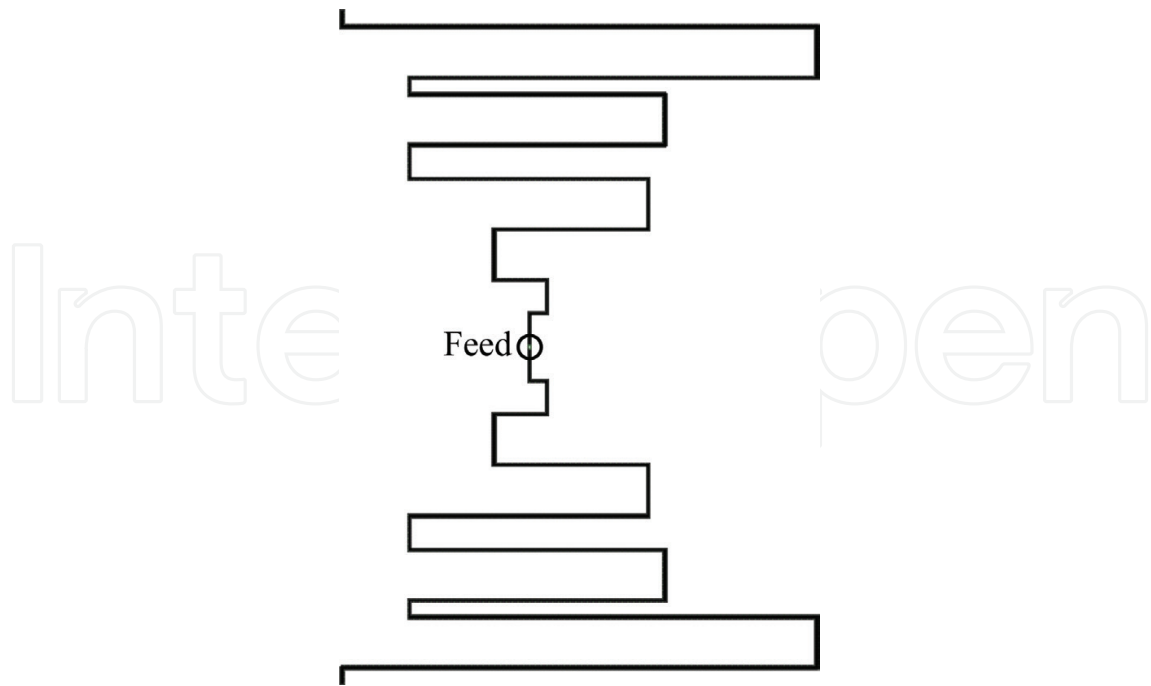
Figure 8. A meander dipole antenna.

(B) Fractal antennas: Fractals are geometrical objects that exhibit a repeating pattern on many different length scales. Very long fractal curves can be fit into a relatively small area. This feature of the fractals, in addition to their self-similarity, attracted antenna engineers and has been used by them to create a new class of antennas, called fractal antennas [5]. The multiband performance and compactness of the fractal antennas make them a good candidate for wearable designs [14]. For example, the Koch fractal geometry can be used to design compact dipole antennas (**Figure 9**).

(C) Reactively loaded antennas: Boundary conditions applied to an antenna can be modified in a way to change its resonance frequency. This can be done by adding a shorting pin or
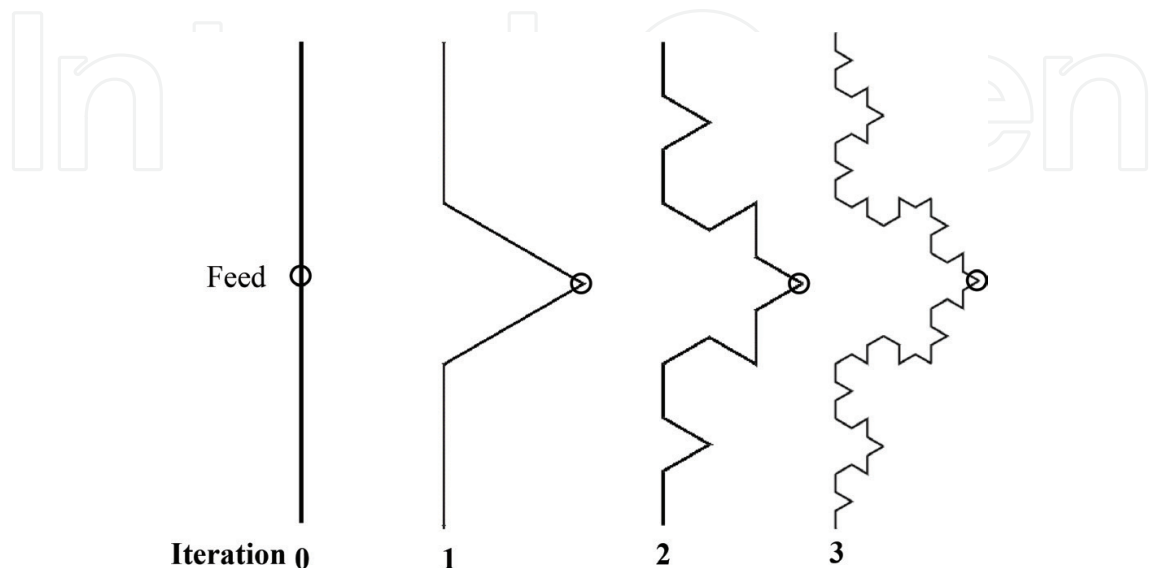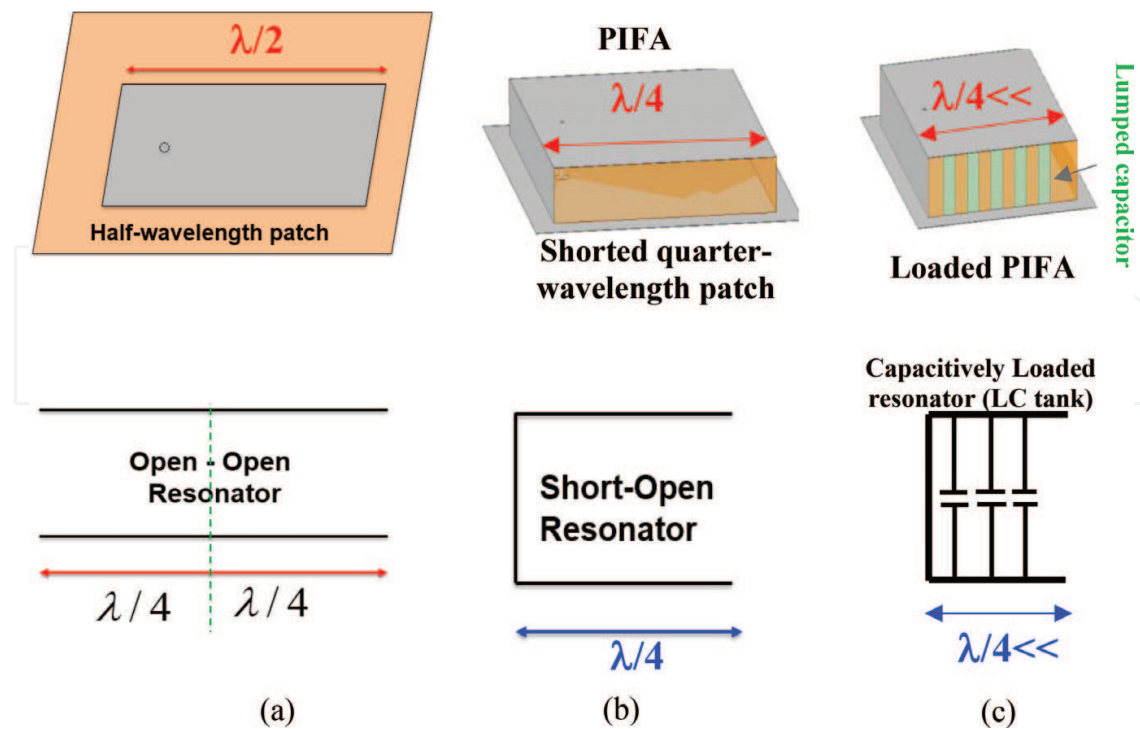

Figure 9. Different iterations of Koch dipole antenna.

Figure 10. Miniaturing a conventional patch antenna: (a) the patch and its resonator model, (b) shorted quarter-wavelength patch (or PIFA) and its equivalent resonator model and (c) loaded PIFA and its resonator model.

loading the antenna with appropriate lumped or distributed inductors or capacitors. For example, a half-wave patch antenna is an open-open resonator (**Figure 10(a)**). By short-ing one of the radiating sides of the patch using a metallic plate or vias, an open-short resonator is created (**Figure 10(b)**). This new resonator can resonate at a lower frequency compared to the open-open resonator. This is the idea behind planar inverted-F antennas (PIFAs). In addition, by loading the nonradiating sides with lumped capacitors, one can create a slow-wave structure and further lower the resonance frequency (**Figure 10(c)**) [5]. This type of antennas can be electrically very small; however, the cost is gain and radiation efficiency degradation.

4. Modeling IEEE 802.11 g wireless network

To establish a successful communication between the wearable device with other wireless devices or the base station (or in general node to node communication), the physical layer provides a backbone, and other layers will be formed on this layer. Having a pervasive simu-lation tool which can combine different modalities and model different layers simultaneously is invaluable to study the wireless communication between nodes. Fortunately, in recent years, there has been significant progress in commercial simulation tools to realize a bottom to top system level modeling and simulation capability. In this section, ANSYS tools will be used to simulate and study the communication between a wearable antenna and a remote node using the IEEE 802.11 g wireless networking standard. Both nodes are assumed to be inside a building (indoor) where the multiple multipath reflections and attenuation makes the wireless communication more challenging.
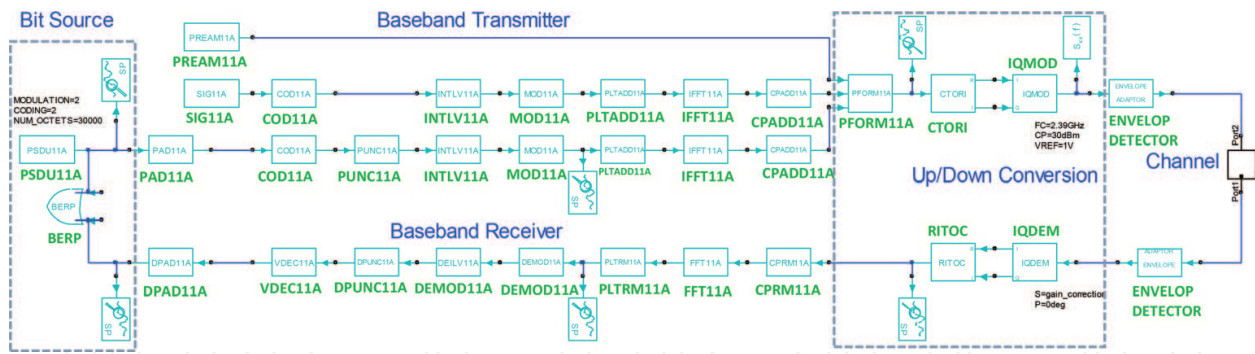
Figure 11. IEEE 802.11 g schematic view inside ANSYS circuit simulator [8].

System-Level Modeling: The entire block diagram for the 802.11 g wireless networking system, available inside the ANSYS Circuit simulator (R18.2), is shown in **Figure 11**. Five different sections can be recognized in this implementation. The source section is responsible for generating the bit stream. The baseband transmitter encodes and modulates the digital bits. The Up/Down conversion section puts the digital signal on a carrier frequency (f_C = 2.4 GHz) in the transmitter side. This section will down-convert the received signal to a baseband signal. The channel represents both transmitter and receiver antennas and the propagation medium between them. In other words, it captures the wave propagation from transmitter to receiver over the wireless communication medium (e.g., building interior).

The channel model can be imported as a scattering matrix [S] from simulation or measurement. For a two-port network (i.e., single transmitter, single receiver), the [S] matrix has four entries ($S_{11}, S_{12}, S_{21}, S_{22}$), and it describes the device/network behavior when it is exposed to the electromagnetic waves. In general, scattering parameters are used to model linear network behavior at high frequencies, and they include valuable information about the device including impedance matching at the ports, insertion loss and delay between the ports. For indoor applications, the environment includes human body, walls, windows, desk, chair, floor and many other objects (**Figure 12**). Therefore, the environment is electrically large, and the chance of multiple and multipath reflections is high. To model such a large problem, the ANSYS Savant tool was used and the communication between the wearable antenna and the wireless node is studied for two
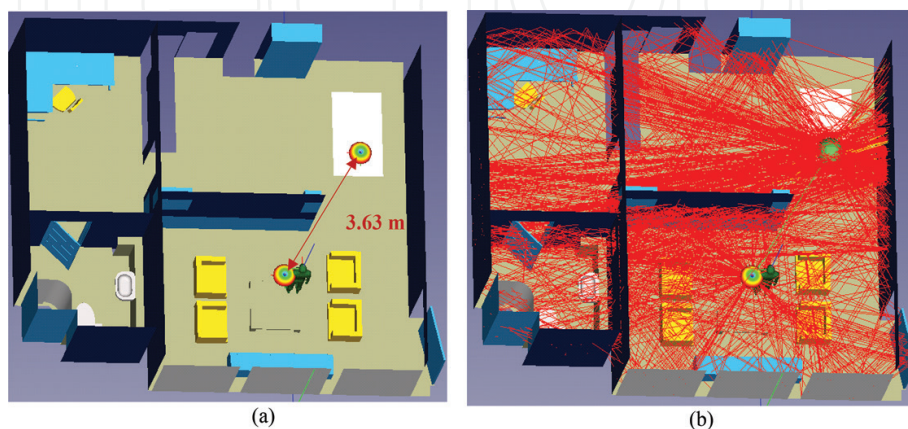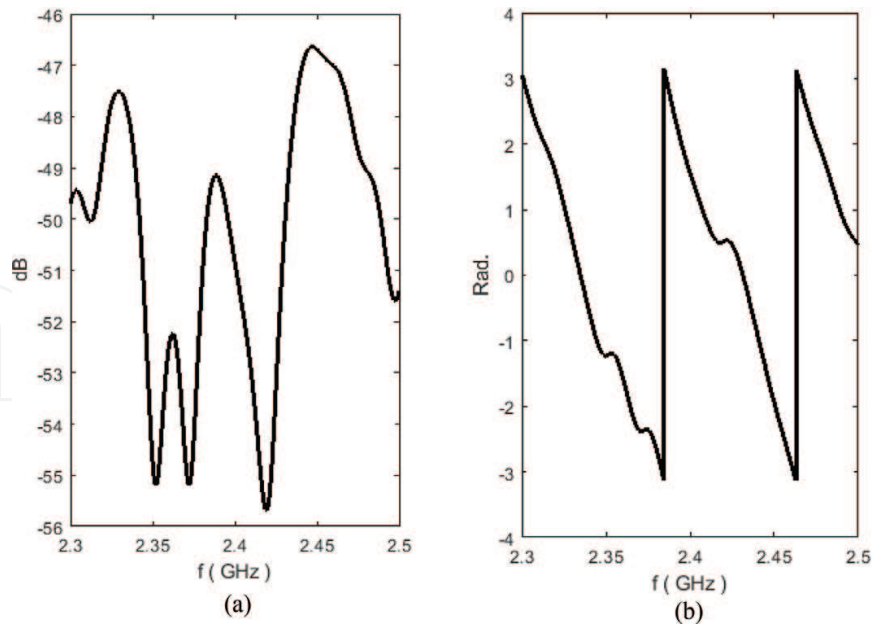

Figure 12. Line of sight indoor communication between wearable device and a remote node modeled in ANSYS Savant: (a) the whole scenario and (b) virtual ray tracing from transmitter to receiver.

Figure 13. ANSYS Savant's simulation result for coupling between the transmitter and receiver nodes for line of sight indoor communication scenario: (a) magnitude in dB and (b) phase in radians.

configurations. For the antennas, half-wave dipoles operating at 2.4 GHz are used. The wearable antenna is called node 1, and the remote external node is named as node 2.

Case 1: In the first scenario, both nodes are positioned at line of sight distance of 3.63 m (**Figure 12(a)**). The simulation was performed in Savant using the shooting and bouncing rays (SBR) technique. The transmitter node (i.e., the wearable antenna) shoots several rays per wavelength. These rays can directly reach to the receiver or arrive with delay after bouncing from the objects (**Figure 12(b)**). The scattering parameter S_{21} (magnitude and phase) which has information about the channel loss/delay is shown in **Figure 13**. Then, the scattering matrix was imported to the ANSYS Circuit simulator and used to simulate the IEEE 802.11 g wireless networking between the nodes. To have a more realistic scenario, white Gaussian noise (WGN) was generated using an external source block, and it was added to the channel's output using sum operator. The carrier
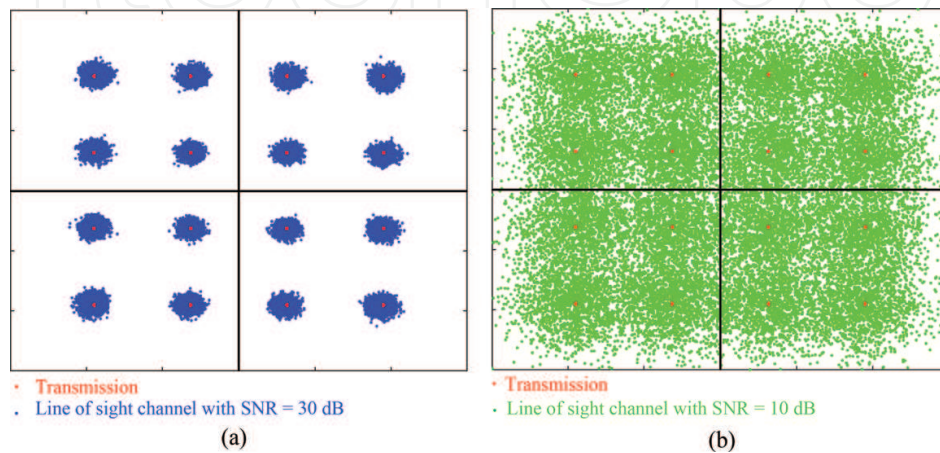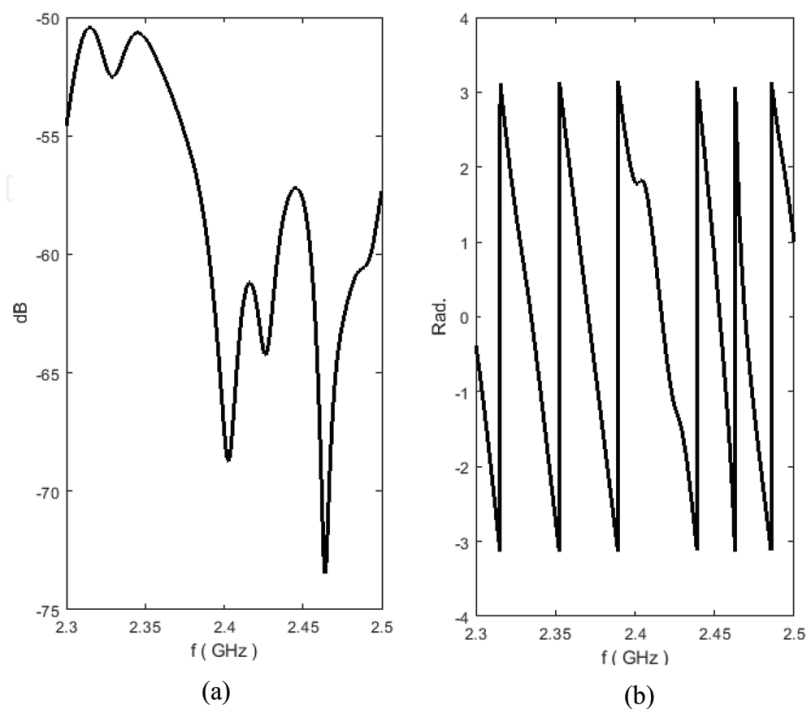

Figure 14. Simulation result for QAM-16 constellation plot at the receiver node for Case 1 (line of sight scenario): (a) SNR = 30 dB and (b) SNR = 10 dB.

signal's power was set to 1 W (30 dBm) and the QAM-16 constellation plot for two different signal-to-noise ratio (SNR) values of 30 and 10 dB are shown in **Figure 14(a)** and **(b)**, respectively. By reducing the SNR to 10 dB, the constellation plot is no longer acceptable.

Case 2: In the second scenario, the nodes are positioned in two rooms separated by walls (nonline of sight scenario) at distance of 7.2 m (**Figure 15(a)**). The rays could only make their way from transmitter to receiver through walls and/or multiple bouncing (**Figure 15(b)**). From the calculated S_{21} in **Figure 16**, it can be seen that the multipath and multiple reflections created an interference pattern and negatively impacted the received signal's strength at the desired frequency range. This shows itself in the constellation plot (**Figure 17**) where the received signals are not categorized properly for SNR as high as 90 dB.

(a)   (b)
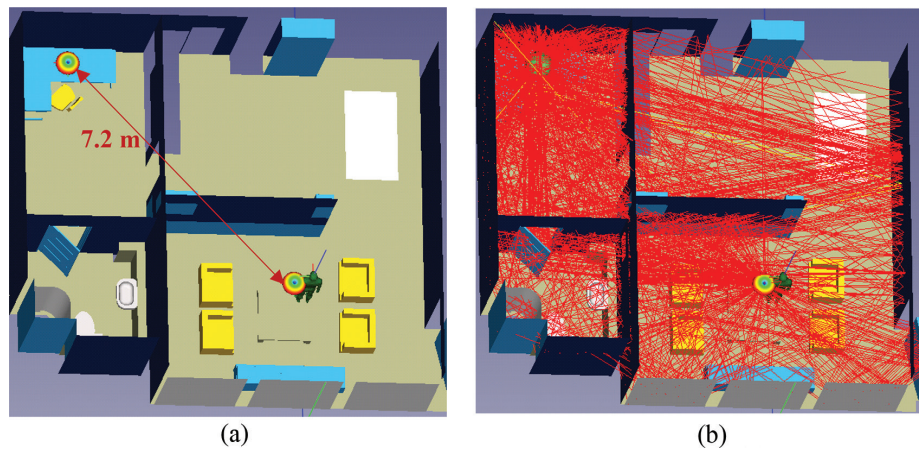
Figure 15. Nonline of sight indoor communication between wearable device and a remote node modeled in ANSYS Savant: (a) the whole scenario and (b) virtual ray tracing from transmitter to receiver.

(a)   (b)

Figure 16. ANSYS Savant simulation result for coupling between the transmitter and receiver nodes for nonline of sight indoor communication scenario: (a) magnitude in dB and (b) phase in radians.
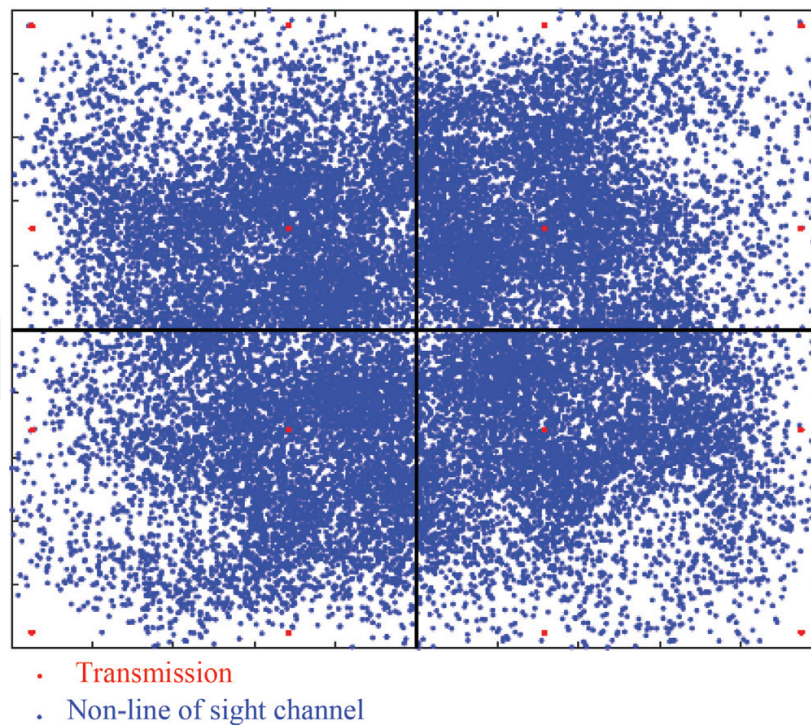
Figure 17. QAM-16 constellation plot at the receiver node for Case 2 (nonline of sight scenario).

5. Summary

In this chapter, some of the issues related to the antenna design and joint modeling of physical and communication layers for wireless body area networking were studied using ANSYS simulation tools. The design of a flexible patch antenna and evaluating its performance near the human body were investigated. Also, for the antenna size reduction, some of the related miniaturization techniques were reviewed. Moreover, a pervasive simulation and modeling idea was used to combine the physical layer simulation results with the communication (and networking) layers. The joint model was used to perform a case study and investigate how the wearable antenna's positioning relative to another wireless node can impact the communication between them for indoor applications.

Acknowledgements

Author details

Mojtaba Fallahpour

Address all correspondence to: mfallahpour@ieee.org

ANSYS Inc., San Jose, CA, USA

References

[1] Movassaghi S, Abolhasan M, Lipman J, Smith D, Jamalipour A. Wireless body area networks: A survey. IEEE Communications Surveys & Tutorials. 2014;**16**(3):1658-1686

[2] Moghadam NN, Farhadi H, Bengtsson M. An energy efficient communication technique for medical implants/micro robots. IEEE International Symposium on Medical Information and Communication Technology (ISMICT'16); 2016

[3] Momenroodaki P, Haines W, Fromandi M, Popovic Z. Noninvasive internal body temperature tracking with near-field microwave radiometry. IEEE Transactions on Microwave Theory and Technique. 2018;**99**:1-11

[4] Momenroodaki P, Popović Z, Fallahpour M. Antenna probes for power reception from deep tissues for wearable microwave thermometry. In: 2017 IEEE International Sympo sium on Antennas and Propagation & USNC/URSI National Radio Science Meeting; San Diego, CA. 2017. pp. 573-574

[5] Fallahpour M, Zoughi R. Antenna miniaturization techniques: A review of topology- and material-based methods. IEEE Antennas and Propagation Magazine. Feb. 2018;**60**(1): 38-50

[6] Fallahpour M, Ghasr MT, Zoughi R. Miniaturized reconfigurable multiband antenna for multiradio wireless communication. IEEE Transactions on Antennas and Propagation. Dec. 2014;**62**(12):6049-6059

[7] Fallahpour M, Ghasr MT, Zoughi R. A multiband reconfigurable CPW-fed slot antenna. In: Proceedings of the 2012 IEEE International Symposium on Antennas and Propaga tion; Chicago, IL. 2012. pp. 1-2

[8] Chen ZN, Liu D, Nakano H, Qing X, Zwick T. Handbook of Antenna Technologies. Singapore: Springer; 2016

[9] www.ANSYS.com

[10] Chahat N, Zhadobov M, Sauleau R. Wearable textile patch antenna for BAN at 60 GHz. In: 7th European Conference on Antennas and Propagation (EuCAP); Gothenburg. 2013. pp. 217-219

[11] https://www.fcc.gov/general/radio-frequency-safety-0

[12] Medeiros CR, Costa JR, Fernandes CA. RFID reader antennas for tag detection in self-confined volumes at UHF. IEEE Antennas and Propagation Magazine. Apr. 2011;**53**(2): 39-50

[13] Amendola S, Milici S, Marrocco G. Performance of epidermal RFID dual-loop tag and on-skin retuning. IEEE Transactions on Antennas and Propagation. Aug. 2015;**63**(8): 3672-3680

[14] Velan S et al. Dual-band EBG integrated monopole antenna deploying fractal geometry for wearable applications. IEEE Antennas and Wireless Propagation Letters. 2015;**14**: 249-252